Mobile Gait Analysis Using Foot-Mounted UWB Sensors

BOYD ANDERSON, National University of Singapore, Singapore
MINGQIAN SHI, National University of Singapore, Singapore
VINCENT Y. F. TAN, National University of Singapore, Singapore
YE WANG, National University of Singapore, Singapore

We demonstrate a new foot-mounted sensor system for mobile gait analysis which is based on Ultra Wideband (UWB) technology. Our system is wireless, inexpensive, portable, and able to estimate clinical measurements that are not currently available in traditional Inertial Measurement Unit (IMU) based wearables such as step width and foot positioning. We collect a dataset of over 2000 steps across 21 people to test our system in comparison with the clinical gold-standard GAITRite, and other IMU-based algorithms. We propose methods to calculate gait metrics from the UWB data that our system collects. Our system is then validated against the GAITRite mat, measuring step width, step length, and step time with mean absolute errors of 0.033m, 0.032m, and 0.012s respectively. This system has the potential for use in many fields including sports medicine, neurological diagnostics, fall risk assessment, and monitoring of the elderly.

CCS Concepts: • **Applied computing** → *Consumer health*; • **Hardware** → *Sensor applications and deployments*; *Wireless devices*.

Additional Key Words and Phrases: Gait Measurement, Ultra Wideband, Inertial Measurement Units

ACM Reference Format:
Boyd Anderson, Mingqian Shi, Vincent Y. F. Tan, and Ye Wang. 2019. Mobile Gait Analysis Using Foot-Mounted UWB Sensors. *Proc. ACM Interact. Mob. Wearable Ubiquitous Technol.* 3, 3, Article 73 (September 2019), 22 pages. https://doi.org/10.1145/3351231

1 INTRODUCTION

Gait analysis is the measurement of quantities related to human locomotion (for example step time, or stride length). These quantities are known as spatiotemporal gait parameters. Variability of these gait parameters is an important diagnostic indicator of health [27], correlating with both quality of life and mortality [36], and is of great interest to both clinicians, and researchers. As such, there exists a multitude of technologies for measuring and quantifying gait, including instrumented walking mats, treadmills, motion capture systems, and wearable sensors (pressure sensitive foot switches or inertial sensors) [25]. These technologies have different strengths and weaknesses, for example instrumented walking mats such as the GAITRite[1] provide both spatial and temporal gait analysis at the cost of requiring a relatively large area for use. By contrast, Inertial Measurement Unit (IMU)

[1]GAITRite, CIR Systems, Inc. https://www.gaitrite.com/

Authors' addresses: Boyd Anderson, NUS Graduate School of Integrative Sciences and Engineering and School of Computing, National University of Singapore, Singapore, boyd@u.nus.edu; Mingqian Shi, School of Computing, National University of Singapore, Singapore, mingqian@u.nus.edu; Vincent Y. F. Tan, Department of Electrical and Computer Engineering and Department of Mathematics, National University of Singapore, Singapore, vtan@nus.edu.sg; Ye Wang, School of Computing and NUS Graduate School of Integrative Sciences and Engineering, National University of Singapore, Singapore, wangye@comp.nus.edu.sg.

2474-9567/2019/9-ART73 $15.00
https://doi.org/10.1145/3351231

based wearable sensors such as the Shimmer3,[2] sacrifice measurement accuracy and comprehensiveness for portability and practicality.

Unlike most walking mats, treadmills, or motion capture clinical gait analysis systems, IMU-based wearable sensors allow for a more convenient and practical way to perform gait analysis outside of a laboratory or hospital setting. As such, these sensors can be used to capture the natural walking of elderly persons or those with neurological conditions. However, some measures of gait variability of clinical interest are difficult to estimate using IMU-based sensors. One reason for this limitation is because the sensors only measure acceleration and rotation and to get even simple gait parameters (such as stride length) complicated models must be employed. One important gait parameter that is difficult to estimate with IMU-based sensors is step width, which is an indicator of fall risk [7, 26]. Another is estimating the placement of the foot in terms of base-of-support during walking, which can help in evaluating balance and subsequently fall risk [19].

One way to expand the capabilities of wearable sensors is the use of time-of-flight ranging technologies. Ultra Wideband (UWB) is a radio technology used primarily for indoor positioning or localisation applications [2]. However, recently due to miniaturisation it has found use in medical fields. UWB can be used to find distances to centimetre accuracy [24]. Supplementing IMU-based sensors with UWB radios could allow wearable sensors to measure both stride width and foot placement in addition to standard gait parameters already calculated by IMU systems. In this work we propose a wearable sensor network using UWB sensors to provide accurate measurements for gait analysis. The availability of inexpensive and accurate UWB devices have allowed us to develop a wearable sensor network with two sensors mounted on each of the left and right shoes. Each UWB sensor measures the distances to two sensors on the other shoe, allowing an accurate assessment of shoe placement relative to the other shoe. Unlike the GAITRite, this placement can be calculated throughout the stride. Our goal is a system which combines the benefits of both instrumented walking mats (spatial accuracy) and IMU-based wearable sensors (portability).

1.1 Contributions

(1) We describe a new wearable wireless sensor system for gait analysis which is based on UWB technology. The main advantage of our system is that it is able to estimate clinical measurements that are not currently available in IMU-based wearables such as step width and spatial foot placement.
(2) We collect and analyse a walking dataset of over 2000 steps across 21 people to compare our system to the clinical gold-standard GAITRite. The dataset includes time-synchronised UWB and IMU measurements, along with ground truth GAITRite measurements.
(3) We propose low computational complexity methods for the estimation of gait metrics using UWB data. We compare these against measurements made on the GAITRite walking mat.
(4) We demonstrate a simple technique of late fusion of IMU and UWB processed data which improves these estimates of gait metrics.
(5) We validate our system against the GAITRite mat, measuring step width, step length, and step time with mean absolute errors of 0.033m, 0.032m, and 0.012s respectively.

The paper is laid out in the following way. The next section discusses related work. Section 3 gives some definitions for important gait metrics used in this paper. Section 4 details the custom sensor system used in this project. In Section 5, the UWB ranging protocol is described. The calibration of the sensors is described in Section 6. System algorithms are explained in Section 7. Section 8 describes the data collection and results. Section 9 discusses the limitations and future work of this project, followed by the conclusions in Section 10.

[2]Shimmer https://www.shimmersensing.com/

2 RELATED WORK

Wearable technology for gait analysis is a crowded, active, and well-published field [9], and there exist multiple commercial clinical and recreational products (see Table 1). Wearable IMU-based sensors are widely used [1], and have been used to record the gait of healthy elderly people, and those with neurological conditions such as Parkinson's Disease patients [13]. These systems can measure many gait parameters, including step time, step length, step time variability and step length variability [41]. However, other gait parameters are harder to estimate reliably such as swing time [13] or step width [30]. Additionally, sensor location [5, 10], speed [10] and the algorithms employed in analysis have a direct effect on the accuracy of any gait parameters estimated.

Indeed, the use of foot-mounted IMUs for gait metric estimation is a common strategy. Foot-mounted sensors can measure heel-strike time, toe-off time, stance time, swing time, cadence, foot clearance, and stride length [11, 37], even amongst those who suffer neurological conditions [3, 37]. Another shoe-mounted system is SpiderWalk, which uses vibration sensors to perform activity detection [38]. This system uses machine learning methods to determine not only the performed activity (such as walking) but also other relevant contexts (such as walking surface). However, it does not calculate any gait metrics such as step length.

Table 1. Some Popular Commercial Gait Analysis Systems

Commercial System	Sensor Type	Sampling Rate	Portability
Shimmer3	IMU	50 Hz -1000 Hz	High
Xsens MVN	IMU	240 Hz	Medium
F-Scan	Pressure Sensor	Up to 750 Hz	High
stt 3DMA	Motion Capture	100 Hz	Low
Vicon	Motion Capture	135 Hz	Low
GAITRite	Walking Mat	Up to 240 Hz	Low

2.1 IMU Gait Algorithms

Gait algorithms are used to analyse data from IMU sensors and estimate gait metrics such as stride length. These methods try to mitigate the errors caused by sensor noise/sensitivity and numerical computational errors. Common methods to overcome these limitations are either the use of Kalman filter-based algorithms [22, 37], machine learning approaches [35, 39], or simple double integration methods [42]. Some of these methods can be used even on the low computational power available to wearable sensors. Others have opted for the use of deep learning approaches, resulting in comparable accuracy to these previously mentioned common approaches [18] though they require large amounts of data. Deep learning has also been used for detecting freezing of gait [8], and gait recognition [12]. These deep learning models however are currently not scalable to embedded system hardware such as those found in wearable sensors. It is also possible to use the raw data from IMU sensors to directly infer gait asymmetry [4] but these methods do not give clinically relevant gait parameters.

2.2 UWB For Wearables

Recently UWB technologies have found use in medical systems due to their low power requirements, non-invasiveness, and the low risk of the technology [15]. Specifically, researchers have used wearable UWB radios to estimate joint flexion/extension angles of the knee and elbow [29]. UWB ranging sensors have been used to do body motion capture [17], body tracking [33], and even track limb movement [6] specifically for health-care related applications. The miniaturisation of this technology now allows for wearable body sensor networks which can perform accurate ranging. Methods for fusion of IMU and UWB have been already considered [23, 40] and

have shown an improvement in stability and accuracy of measurements for localisation but have not considered the problem of human locomotion.

The most related system [14, 32] that looked at the use of UWB for measurement of gait parameters (specifically step width) used a bulky oscilloscope and signal generator system making it not portable or practical. However, as a proof of concept this system provided a new approach to using UWB for gait measurement. Additionally, the location of the UWB sensors was limited to only the back of the heels, and whilst this is good for the measurement of step width it gives no information on foot placement location. Our proposed system uses IMU and UWB Integrated Circuits (ICs) in combination with algorithms to estimate gait parameters currently not measurable by IMU-based sensors alone.

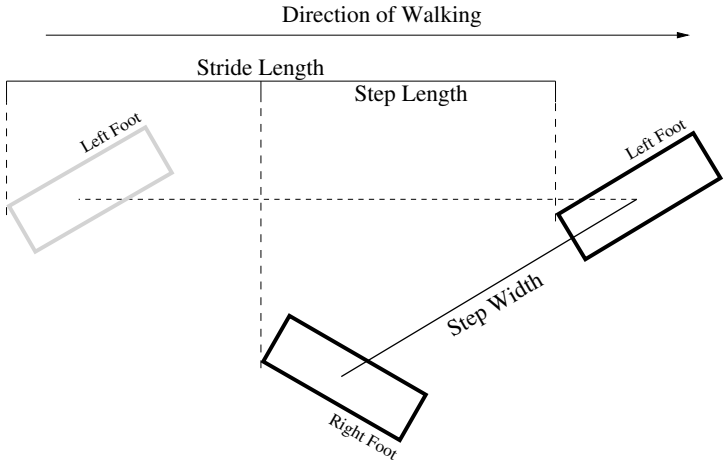

Fig. 1. Spatial Gait Metric Definitions.

3 GAIT DEFINITIONS

For direct comparison with the GAITRite walking mat, we will use their (commonly accepted) definitions for some important gait metrics. When one foot is off the ground this is known as *single support time*, and when both are on the ground this is known as *double support time*. A *heel strike* is defined as the time the heel of the foot makes contact with the ground. Likewise, a *toe off* is defined as the time the toe of the foot leaves contact with the ground. From these definitions, we can derive the following gait metrics:

- *Step Time* is the duration between two heel strikes of alternating feet.
- *Step Length* is the distance (in direction of movement) between two consecutive placements of alternating feet.
- *Step Width* is the diagonal distance between the mid-point of the feet during double support time.
- *Stride Time* is the duration between two consecutive heel strikes of the same foot.
- *Stride Length* is the distance between two consecutive placements of the same foot.
- *Stride Velocity* is the ratio of stride length to stride time.
- *Cadence* is the number of steps made in a fixed time period (commonly measured in steps per minute).
- *Swing Time* is the duration spent during the swing phase (when the foot is not in contact with the ground).
- *Stance Time* is the duration spent during the stance phase (when the foot is in contact with the ground).

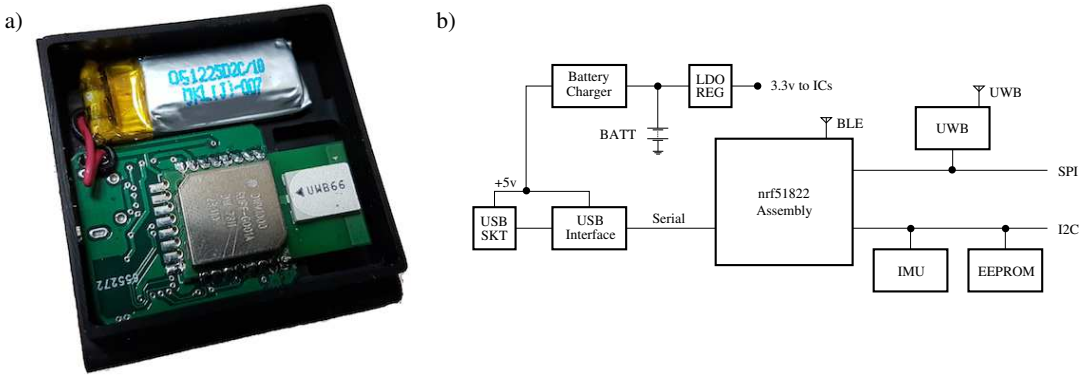

Fig. 2. PCB Sensor in open case, and block diagram.

These metrics and the variability of them are all useful to clinicians for diagnosis of neurological conditions or in evaluating general health. With these definitions in place (see Figure 1 for an overview of the spatial metrics), we now move to the custom-built system that was used in this paper.

4 SYSTEM SPECIFICATIONS

The goal of this project is to build a system to measure gait metrics that are currently only possible on treadmills, motion capture systems, and walking mats (such as *Step Width*) using wearable sensors. Therefore we choose a configuration of sensors on the feet in a very specific way. Our system consists of four foot-mounted IMU/UWB sensors which connect to a smartphone application using Bluetooth.

The custom built units (see Figure 2a and 2b) were designed with measuring human motion in mind. They have a core nrf51822-based assembly with a 32-bit ARM Cortex M0 at 16MHz, with 24kB of RAM, and 128Kb of flash memory. In addition, on board they have a 6-axis IMU MPU6050 providing three channels from an accelerometer (a_x, a_y, a_z) and 3 channels from a gyroscope (g_x, g_y, g_z). The system also has a real-time location module, the DWM1000. This module can be used for absolute range measurements. The ranging sensor is configured with a transmission rate of 6800 Kbps, and a pulse repetition frequency of 64 MHz. In terms of standard connectivity, the sensor supports Bluetooth 4.2 (BLE) and USB. The sensor has 256kB of EEPROM, and it includes battery management circuitry to support ultra low power use cases, and measuring and charging the attached 110mAh LiPo battery. The unit is a single-sided 20.4mm × 24.1mm PCB and has a case for mounting on a shoe. These sensors can be used to measure distances as well as motion. The configuration of the sensors and their locations on the body determine what measurements can be extracted.

4.1 Sensor Configuration

Four sensors are mounted on a pair of shoes. We will designate them u_1, u_2, u_3 and u_4, such that u_1 and u_2 are on the right shoe and u_3 and u_4 are on the left (see Figure 3a). The first sensor (u_1 or u_3) is flat on the front toe area and the other (either u_2 or u_4) vertically oriented on the heel as in Figure 3b. Therefore, the distance between the front of the two shoes (u_1 and u_3), is defined as $\overline{u_1u_3}$. Sensors on either foot are a fixed distance away from each other (L the length of the shoe), and as a result these distances are not measured. These four measurement distances $\overline{u_1u_3}$, $\overline{u_1u_4}$, $\overline{u_2u_3}$, $\overline{u_2u_4}$ and the fixed length L make up a rigid irregular quadrilateral between the feet (see Figure 11). The polygon defined by these measurements will allow us to calculate the step (and stride) length

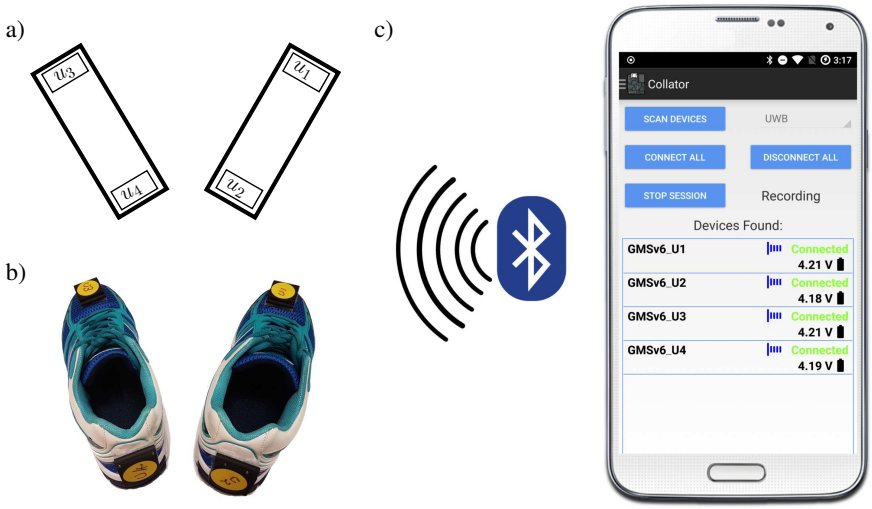

Fig. 3. Components of the system: Shoe sensors, and linked smartphone application.

and width, and the placement of the shoes relative to each other in Section 7. The sensors transmit the following data at a sampling rate of 100Hz:

- Timestamp in milliseconds (t)
- 3 axes of Acceleration (a_x, a_y, a_z)
- 3 axes of Rotation (g_x, g_y, g_z)
- 2 distance measurements ($\overline{u_1u_3}$ and $\overline{u_1u_4}$ or $\overline{u_2u_3}$ and $\overline{u_2u_4}$)
- Sensor temperature (T_x)

This data is sent over Bluetooth to a smartphone running a collating application (see Figure 3c) attached to the body. This application, known as the Collator, connects to and controls the system over Bluetooth. Each walking session is initiated on the smartphone and then the app decodes and saves the raw data for later processing. For best line of sight, the UWB aerials of each sensor are pointed inwards towards the other shoe. As the back of the heel has been found to be an optimum place to position an IMU for gait measurement [5], the sensors on the back of the heels are the only ones which we will use to measure acceleration and angular speed. The orientation of this sensor and its channels can be seen in Figure 4.

4.2 Device Synchronisation

In order to accurately describe the motion of the feet we need to have a high sampling rate. The system currently records IMU and UWB measurements on all four sensors at 100 Hz, time-locked to within a few hundred μs. However, this high sampling rate needs to be balanced with the power efficiency concerns of any wearable technology. To achieve this, the four sensors need to know precisely when they should turn on their UWB radios for any communication required. The strategy for this synchronisation, is that in every ten millisecond interrupt, a "beacon" message is sent (after a constant delay into the interrupt) from only one of the sensors. This beacon message is used by the other remaining sensors to move their interrupt timings in-line with the beacon. Over a few hundred milliseconds, all devices become locked to this beacon pulse to within μs. Therefore, the timings of any potential ranging protocol are known to all of the devices, meaning that the UWB radios are turned on or off

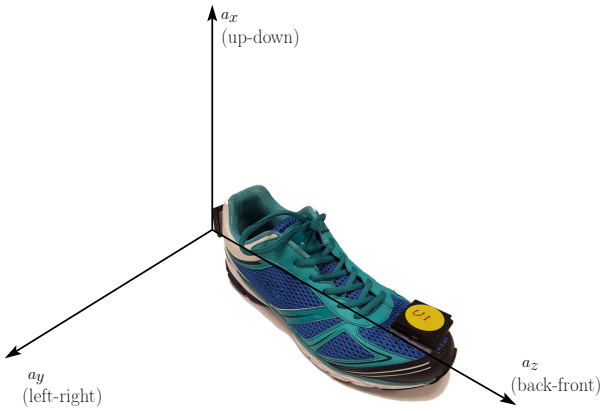

Fig. 4. IMU channel orientation with respect to the shoe.

as required. This allows the system to reduce its power consumption and improve efficiency by only turning on the UWB radios approximately 20% of the time.

4.3 Power Consumption

To test the power efficiency of our system we run two experiments. In the first experiment, we attempt to emulate the worst-case use case, the system being used for continuous recording at 100Hz. We find that under continuous operation, the system lasts 2.5 hours, as can be seen in Figure 5a. It is possible to see that the system stops working after u_2 is battery depleted. In a clinical gait assessment, the use case is not continuous. Each session takes approximately 10-15 minutes, and therefore we would be able to assess ten to fifteen subjects on one charge. The second experiment was the long-term standby mode, as can be seen in Figure 5b. Under this condition, the sensors can last at least fifty days in standby mode.

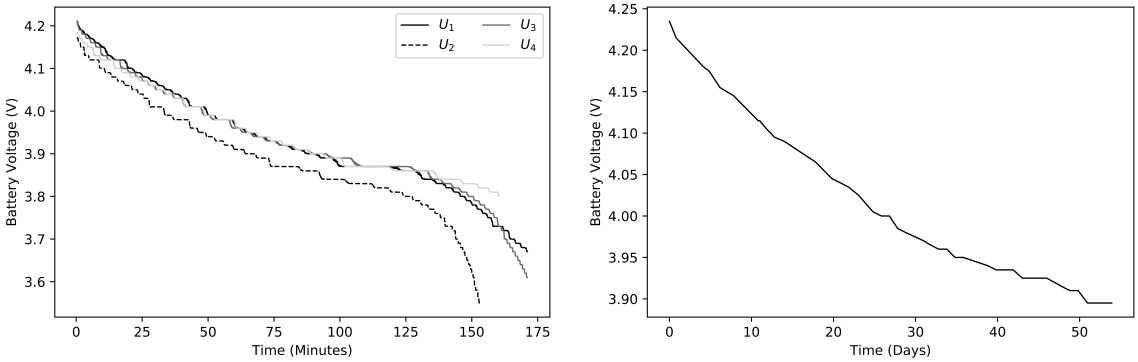

(a) Continuous use case

(b) Long-term standby use case

Fig. 5. Battery characteristics of sensor systems under two different use cases, continuous use, and long-term standby mode.

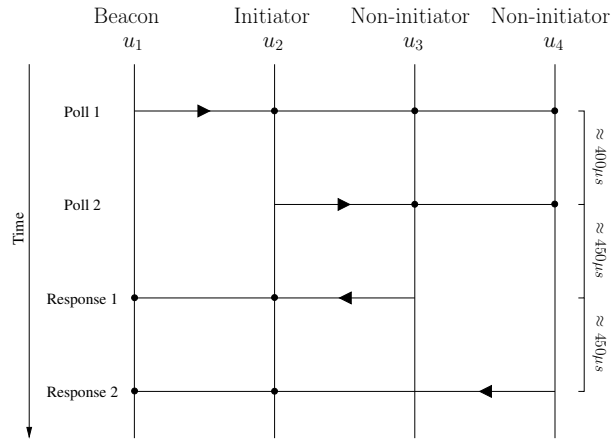

Fig. 6. UWB Ranging Protocol Diagram.

5 RANGING PROTOCOL

The traditional designations for devices in most studies of UWB are the terms *anchors* and *tags*, as some devices are in fixed locations (anchors) and are used to localise other moving devices (tags). This definition does not make sense in our configuration as all devices are moving. We will adopt the following terms, *initiators* and *non-initiators*. Initiators begin the ranging protocol, and non-initiators reply to these requests. The initiator that starts the protocol is the *beacon* as it will broadcast (and hence dictate) the current time to all other devices.

The sensors on the right shoe (u_1 and u_2) behave as *initiators* and the other two (u_3 and u_4) behave as *non-initiators*. As our sensor has to sample the onboard IMU and transmit a Bluetooth packet within each ten ms interrupt, we have to work with a very limited time budget, only a two ms window to do the entire UWB ranging protocol. Were it not for these time constraints, we would be able to run this ranging protocol at 200-500Hz, albeit with a much higher power consumption. The standard approach is a symmetric double-sided two-way ranging protocol, where the protocol is structured to remove the errors caused by the different relative speeds between device oscillators/clocks. However, this approach requires more messages and a much larger time budget. Therefore, we use a custom single-sided two-way ranging protocol with poll and response messages. To speed up the protocol, only the initiators compute a distance measurement. The protocol involves four messages:

(1) **Beacon (u_1)** Poll 1: 7 byte message containing beacon time and requesting a range
(2) **Initiator (u_2)** Poll 2: 3 byte message requesting a range
(3) **Non-initiator (u_3):** Response 1: 11 byte message containing the time in 15.65 picosecond increments between the received poll messages from u_1 and u_2, and this response message
(4) **Non-initiator (u_4):** Response 2: 11 byte message containing the time in 15.65 picosecond increments between the received poll messages from u_1 and u_2, and this response message

The ordering of these transmission steps can be seen in Figure 6 and 7. These Poll and Response messages give us the required timestamps for ranging as can be seen in Figure 8. This protocol takes approximately 1.8 milliseconds, and is performed 100 times a second. After receiving a response, the initiators calculate the duration from sending a poll message to receiving the response message ($t_{Rx} - t_{Sx}$) and then these timestamps are used for calculating the time-of-flight (t_{xy}) between u_x and u_y, and as a result the distance between them. The formula is,

$$t_{x,y} = \frac{(t_{Rx} - t_{Sx}) - (t_{Sy} - t_{Ry})}{2},$$

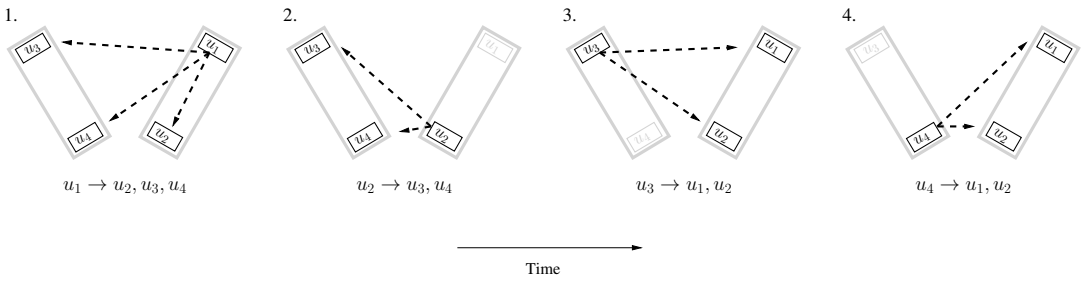

Fig. 7. UWB Ranging Protocol Steps.

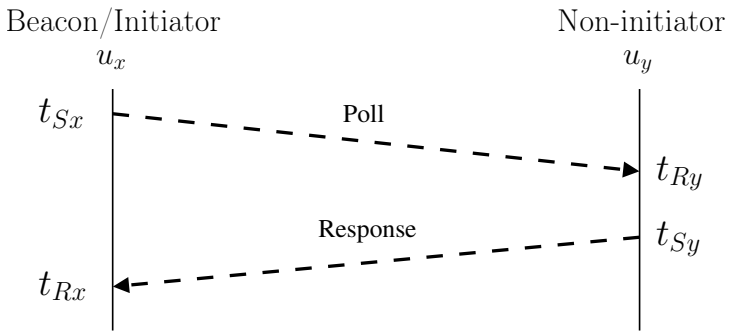

Fig. 8. UWB Ranging Poll-Response Diagram.

and the distance between sensor u_x and u_y is therefore,

$$\overline{u_x u_y} = c t_{x,y},$$

where c is the speed of light. Radio transmissions such as our UWB signal, propagate at c, the speed of light in a vacuum. However, through any other medium (such as air), these signals propagate slower depending on the refractive index of the medium. In practice, this difference is negligible, typically of the order of 0.03%, and therefore we use c in the above equation. These time differences are made with respect to the different oscillators on each device and as a consequence they can be (and are) not exactly in sync. Additionally, there are errors associated with antenna delay and manufacturing differences in the DWM1000 chip, and as such the UWB ranging sensor needs to be calibrated. First however, we will investigate the relationship between sensor distance and measurement variation.

5.1 Measurement Variation

Due to UWB being mostly used for localisation, the official Decawave datasheet[3] makes the commonly repeated accuracy claim that the devices have a precision of 10 cm ("asset location to a precision of 10 cm"). This reported figure is pessimistic for our use as it is representative of the chip's capabilities over a much larger range (for example 10 to 100 metres). We also note that others [31] have reported that as the distance between transmitter and receiver increases, the variation of the root-mean-square delay spread increases. There are multiple reasons for this, which will be explained in the next paragraph. In order to empirically test this behaviour in our sensors,

[3]DW1000 Datasheet, Decawave, Version 2.09

we measured the variation of our UWB transmissions. This trend can be seen in Figure 9. Note that as the sensors move further away from each other the variation increases. Over the smaller range we are considering in this work, we observe a standard deviation of less than 4.5 cm.

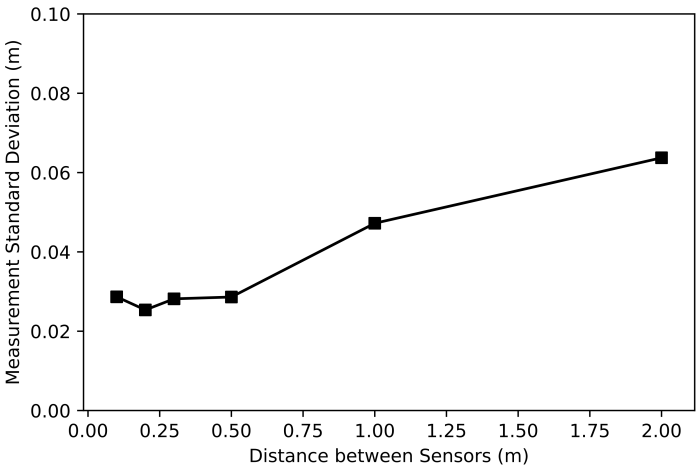

Fig. 9. Measurement Standard Deviation as a function of Distance.

The time resolution of the oscillator in the chip measures in units of approximately 15.65 picoseconds, thus the theoretical smallest distance that is possible to measure is 4.7 mm. However, in practice the capture registers for the incoming transmissions will be dependent on the slope of the rising edge of the received signal. Due to the proximity of the transmitter and receiver, the 'rising edge' of the signal received is much sharper and pronounced. This means it is easier to determine exactly when a transmission arrives and thus reduces the error when calculating the time-of-flight. At larger distances this rising edge becomes less prominent due to a weaker signal, and dispersion, and therefore adds ambiguity to time-of-flight times. Another factor which contributes to this reduction in variation is that over these short distances there are no or minimal reflections. For these reasons, UWB is capable of measuring stable measurements when used over a smaller range. Furthermore, in the algorithm detailed in Section 7, we take approximately 10-15 measurements during the stance phase of walking (i.e. 10-15% of the time at 100Hz) which leads to a better point estimate of each calculated gait metric, further improving the system accuracy. With this set of empirical results, we now turn to the calibration of both the UWB and IMU chips.

6 SENSOR CALIBRATION

Our system has two main chips which require calibration; the UWB and IMU ICs.

6.1 UWB Calibration

There are multiple sources of error in ranging estimation, but here we will concentrate on two main ones. Firstly, the antenna delay of the device. Antenna delay is the internal delay of the chip, and it is determined by the differences in the shape of the aerial and the device temperature. The ranging error can be as much as 2.15 mm per degree centigrade.[4] Due to the problems associated with a single-sided two-way protocol [16, 21], we need to

[4]Application Note (APS013), Decawave, Version 2.2

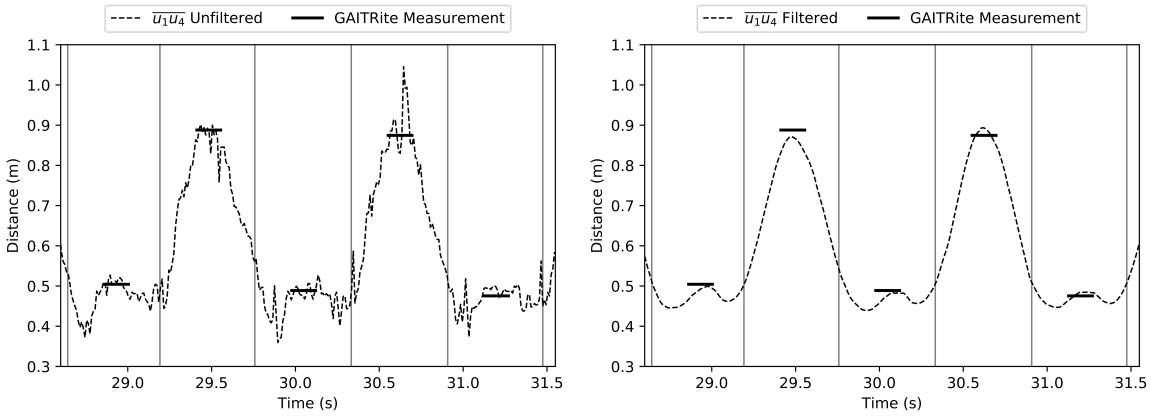

(a) Raw Unfiltered UWB Signal

(b) Savitzky-Golay Filtered UWB Signal

Fig. 10. Both unfiltered and filtered calibrated UWB measurements for $\overline{u_1u_4}$ compared to GAITRite measurements.

compensate for the differences in the oscillator drift.[5] The oscillator has a warm up time and is also affected by device temperature. Any calibration model must compensate for these factors.

Calibration is performed by comparing known distances with UWB measurements. A linear model is fitted to the calibration data to compensate for any error associated with the geometry of the sensor arrangement, the antenna delay, and oscillator differences. The calibrated measurement between device x and y is:

$$\overline{u_xu_y}_{calib} = \rho_0\overline{u_xu_y} + \rho_1(T_{xmax} - T_x) + \rho_2(T_{ymax} - T_y) + \rho_3,$$

where T_x is the temperature of device x, T_{xmax} is the maximum temperature device x reaches at steady state and ρ_0, ρ_1, ρ_2, and ρ_3 are model parameters. UWB walking data corrected using this fitted model can be seen in comparison with the direct measurements from the GAITRite in Figure 10a and 10b. In the second peak of Figure 10a, we can see a spike at the apex, this is likely due to the sensors losing line of sight due to the positioning of the feet. However, this effect is lessened by the use of a Savitzky-Golay filter as can be seen in Figure 10b. Note that in both the raw unfiltered and filtered figures, the maximum and minimum peaks line up with the GAITRite measurements.

6.2 IMU Calibration

In order to get accurate measurements of acceleration we need to calibrate the IMU IC. The MPU6050 uses MEMS (Microelectromechanical systems) for the accelerometers and gyroscopes. As these are physical systems, they have slight manufacturing differences, and therefore these MEMS units vary from one another, and thus require individual calibration, primarily to correct the "zero points" for each axis. A factory calibration is done which sets trim values, but we recalibrate each unit as this factory calibration is not always reliable.

To calibrate each unit, they are held in a particular orientation such that the accelerometer directions for two channels are perpendicular to, and the other channel is co-linear with, the gravitational field of the earth. The units are operated for 10 minutes to achieve a constant temperature, and then tens of thousands of readings are made using MPU Offset Finder code.[6] This program resets a window of trim offsets until each axis moves to the correct values for this orientation. For example, with the Z axis (perpendicular to the IC) pointing down, it should

[5] Application Note (APS011), Decawave, Version 1.0

[6] Robert R. Fenichel's open source project MPU Offset Finder, http://www.fenichel.net/

record exactly 1g. Trim offsets are changed until they read $(a_x = 0, a_y = 0, a_z = 1, g_x = 0, g_y = 0, g_z = 0)$. The final trim offset values are preloaded into the device each time it is used.

7 GAIT METRIC ALGORITHMS

In this section, we will use UWB and IMU measurements to calculate common gait metrics.

7.1 Gait Metrics from UWB Measurements

In order to interpret the signals coming from the UWB sensors, we have to consider the geometry of the arrangement of our sensors, and how they change over time. During the *double support time* (both feet on the ground), we can see that the Heel-Heel distance is given by $\overline{u_2u_4}$, and the Toe-Toe distance $\overline{u_1u_3}$. The maximum Toe-Heel distance (Toe-Heel Max) in this example is given by $\overline{u_2u_3}$ and the minimum Toe-Heel distance (Toe-Heel Min) is given by $\overline{u_1u_4}$. This is because it is a left step and these will be reversed in the right step. Therefore, the maximum and minimum Toe-Heel points are a good proxy for step indicators.

Now, let's consider the change in these measurements in motion. Unlike the GAITRite, this system has the potential to measure the step width whilst the foot is in the air. In Figure 13, we can see the general behaviour of the measured step lengths, note that the minimum Toe-Heel distance and maximum Toe-Heel distance swap after every step. Furthermore, in mid step, we see all of the measurements get smaller as the left foot approaches the other. This minimum is a good proxy for the midway point of the stride.

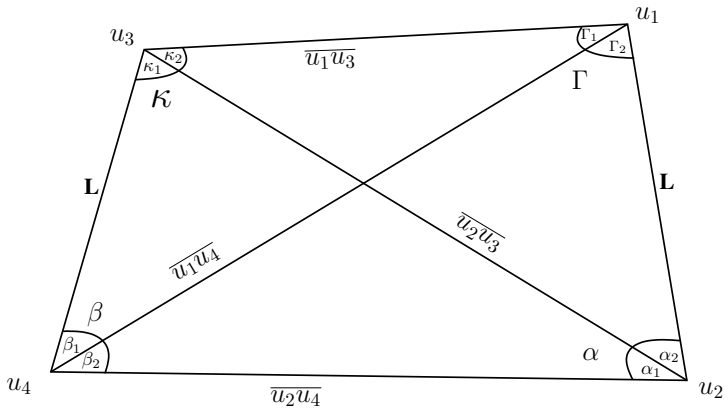

Fig. 11. Irregular quadrilateral (or trapezium) present between the two shoes.

Before performing any calculations on the UWB signals, we first use our UWB calibration function to correct for measurement error. Next, we filter the signal using a Savitzky-Golay filter. This filter was chosen as it would not greatly distort the shape of the signal but still smooth out some of the noise. A continuous wavelet transformed-based peak detection algorithm is used to find the peaks in all four signals. This set of four peaks represent our best estimate of the foot positioning at every step. A sample of two steps is provided in Figure 14. Note, as expected the Heel-Toe Max and Heel-Toe Min swap between $\overline{u_1u_4}$ and $\overline{u_2u_3}$. We also have the internal angles of the irregular quadrilateral present between the two feet as seen in Figure 11, which can all be found using the cosine rule, and are shown below.

$$\beta = \arccos \frac{\overline{u_2u_4}^2 + L^2 - \overline{u_2u_3}^2}{2\overline{u_2u_4}L},$$

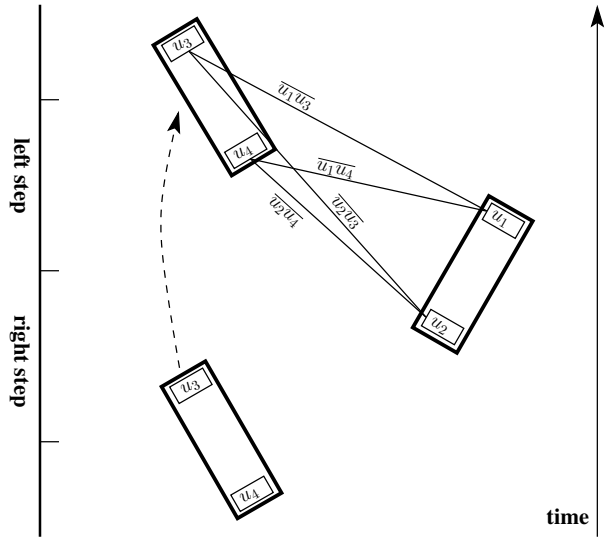

Fig. 12. Demonstration of the UWB measurements after the left step.

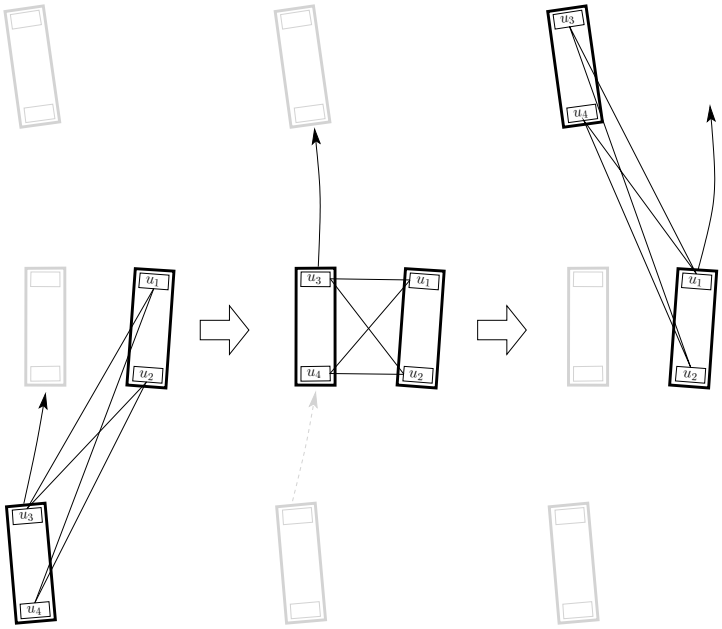

Fig. 13. General behaviour of the ranging system during a step.

$$\kappa = \arccos \frac{\overline{u_1u_3}^2 + L^2 - \overline{u_1u_4}^2}{2\overline{u_1u_3}L},$$

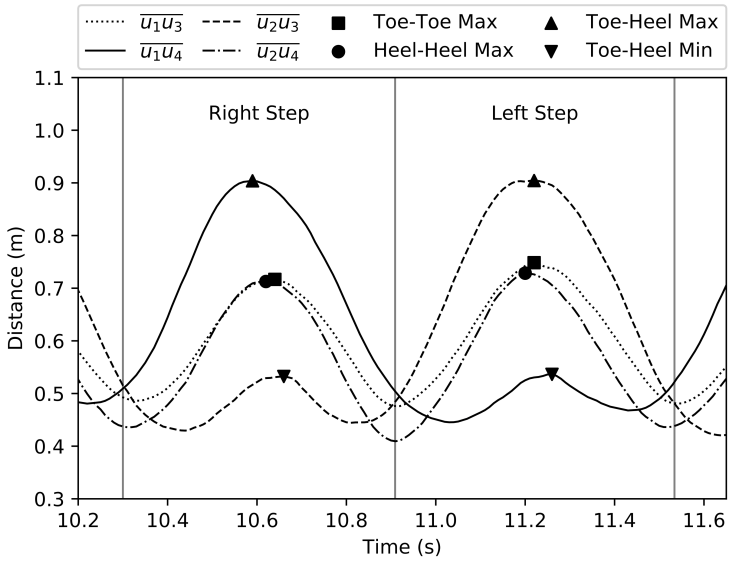

Fig. 14. Annotated example of UWB signal. Vertical lines represent GAITRite step times.

$$\Gamma = \arccos \frac{\overline{u_1u_3}^2 + L^2 - \overline{u_2u_3}^2}{2\overline{u_1u_3}L},$$

$$\alpha = \arccos \frac{\overline{u_2u_4}^2 + L^2 - \overline{u_1u_4}^2}{2\overline{u_2u_4}L}.$$

It is therefore possible to calculate some important gait metrics using these measurements and angles. First, the *step time* (Stp_t) is defined as the difference of two consecutive alternating Heel-Toe maximums, and the *stride time* (Str_t) is the sum of two consecutive *step times*. Stance time can be calculated based on the proportion of time that the UWB signal spends above an empirically defined threshold (time spent at the top of the Heel-Toe peak), and swing time is just the rest of that proportion. Cadence can be calculated by counting the number of Heel-Toe maximums in a fixed duration. The step length is defined as the component of $\overline{u_2u_4}$ in the direction of walking,

$$Stp_l = \overline{u_2u_4}\cos\beta_2 \quad \text{or} \quad \overline{u_2u_4}\cos\alpha_1,$$

for the right and left steps respectively, where the angles β_2 and α_1 are defined as

$$\beta_2 = \arccos \frac{\overline{u_1u_4}^2 + \overline{u_2u_4}^2 - L^2}{2\overline{u_1u_4}\ \overline{u_2u_4}} \quad \text{and} \quad \alpha_1 = \arccos \frac{\overline{u_2u_3}^2 + \overline{u_2u_4}^2 - L^2}{2\overline{u_2u_3}\ \overline{u_2u_4}}.$$

The stride length Str_l is defined as two consecutive step lengths. The step width is defined as the distance between the two mid points of the feet which by geometry is,

$$Stp_W = \frac{\overline{u_1u_3} + \overline{u_2u_4}}{2}.$$

Furthermore, we can calculate the stride velocity as

$$Str_V = \frac{Str_l}{Str_t}.$$

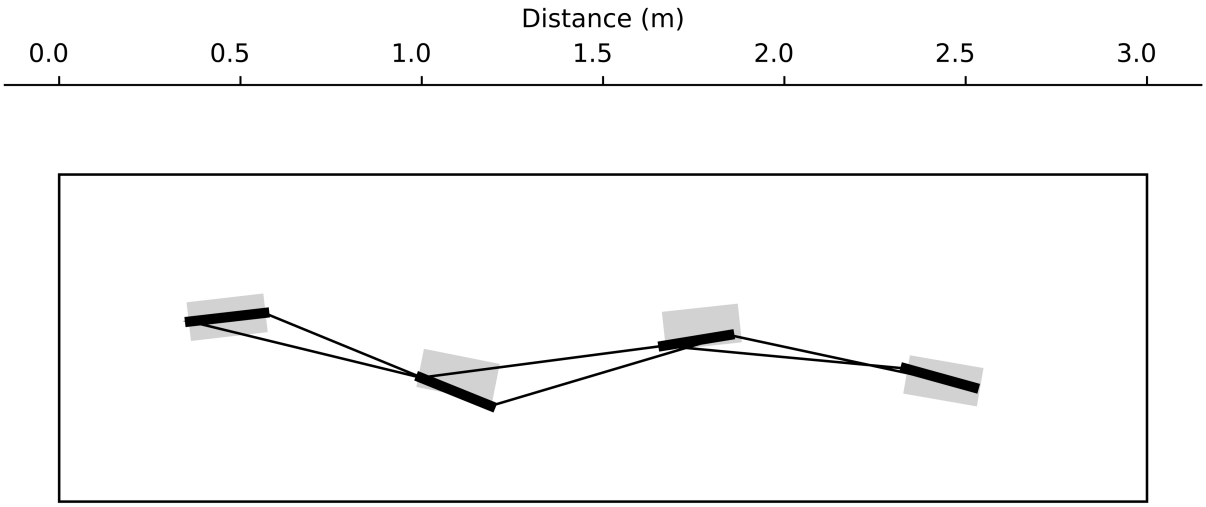

Fig. 15. A plotted trajectory of alternating steps. Gray rectangles are the steps as measured by the GAITRite.

Additionally, with these angles it is possible to calculate the positioning of the feet (relative to each other).

Next, we will compare the foot placement of our system with the foot placement of the GAITRite mat. To do this, we anchor our system spatially to the first foot of the GAITRite. In Figure 15 we can see the spatial capabilities of our system. It shows the plotted trajectory of three steps of a walk, where each irregular quadrilateral is taken from the Heel-Toe maximum point. The gray footprints in the figure show the GAITRite foot positioning. The thick black lines represent our systems best estimation of foot placement. Even though the angles calculated between these measurements are at their least accurate at this point (due to some sensors not having direct line of sight) it is still possible to calculate these step locations. Note, that the walk is straight and does not drift to either side, as can be seen in IMU-based sensors. Importantly, all of these calculations are low complexity enough that they could be run on embedded hardware. In the next subsection we will look at the IMU data in isolation, and use two methods to estimate stride lengths and times.

7.2 Gait Metrics from IMU Data

The raw IMU data is linearly interpolated, re-sampled at 1000 Hz, and then low-pass filtered with a cutoff of 10 Hz (to remove noise), as is common in similar IMU studies [43, 44]. With this cleaned and interpolated data, we now turn to the problem of estimating stride length. As our system does not include a magnetometer, it is very difficult to orientate the sensors with respect to each other, and therefore does not consider the estimation of step length using only IMUs. In this paper, we use a simple (and low computational cost) zero-velocity update double integration method, based on using the gyroscope to compensate for the change in orientation of the sensor during walking. These methods were picked as they can be run on embedded hardware.

As our sensor is oriented such that all three accelerometers are approximately in line with the three planes of the body, we can use the following general definitions: a_x is the acceleration up-and-down a_y is the acceleration left-to-right, and a_z is the acceleration back-to-front. Figure 16 shows an example of the IMU data recorded during walking, and it is taken from the same two steps as in Figure 14. In general, we can see most of the acceleration occurs in the up-down (a_x) and back-front (a_z) directions, and this intuitively makes sense in the context of walking. We can also see the dominant rotation around the left-right axis (g_y). This is the ankle rotating during a walk.

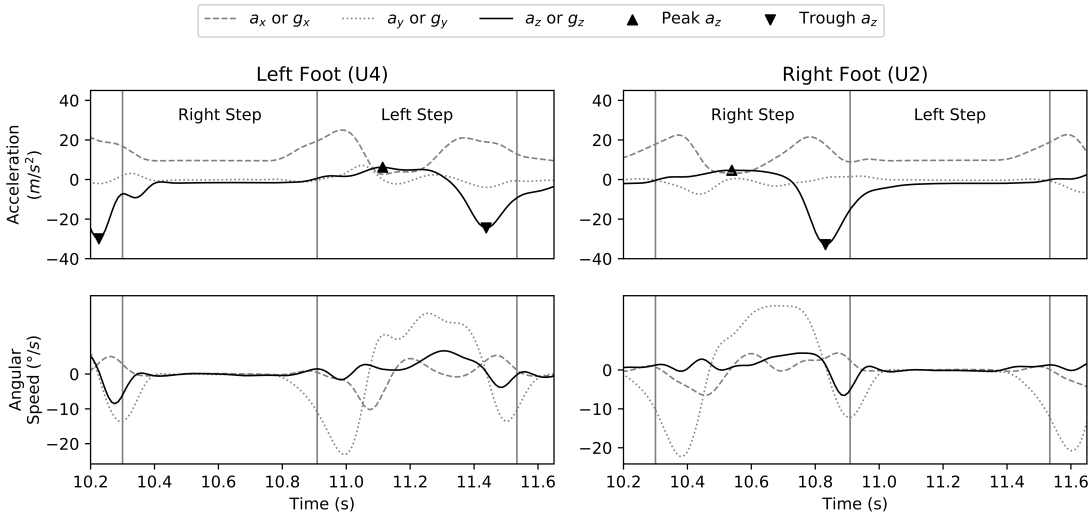

Fig. 16. Annotated example of IMU signal. Vertical lines represent GAITRite step times.

The first stage of the algorithm involves finding the peaks and troughs in a_z. These peaks are analogous to the toe-off and heel-strike events that occur during walking. The stride time can therefore be defined as the distance between two consecutive peaks. The stride length is defined as the double integral of the acceleration in the forward direction. However, due to the rotation of the sensor, the channels of acceleration cannot be used directly.

The first model involved using the gyroscope g_y, to compensate for the rotation of the ankle. Using this method, the acceleration in a_x and a_z is combined into a vector based on the angle of rotation. The method only uses 3 axes of the IMU. Another approach is to use all 6 axes of the gyroscope and accelerometers to compensate for the 3D motion of the foot. As before these IMU readings are transformed from the IMU reference frame, into a global reference frame, this time using the method based on the Direction Cosine Matrix (a full description of this methodology can be found in [28]). Once these transformed values are found, the signal is integrated twice between the consecutive peak and trough, this being the stride length. Now, with a complete and calibrated system, and a set of algorithms, we collect some walking data of healthy adults and compare against the "gold standard" clinical device [20], the GAITRite walking mat.

8 SYSTEM EVALUATION

In this section, we describe the dataset collected for this paper, and report the performance of our gait measurement algorithms on this dataset.

8.1 Dataset

Walking data from twenty one healthy adults (between the ages of 21 and 35), were recorded concurrently with a GAITRite walking mat and our sensor system. The GAITRite walking mat is capable of measuring stride time, step time, stride length, step length, stride width, and step width amongst others and is therefore a good choice to serve as our ground truth measurement and as a comparison to our system. GAITRite claims a spatial resolution accuracy of ±1.27cm.[7] Each subject walked on a walking track for more than 80 steps, split up into 15 "sessions",

[7]GAITRite Electronic Walkway Technical Reference, CIR Systems Inc., WI-02-15 Revision L

defined as one walk over the mat. All data was collected with the approval of the National University of Singapore Institutional Review Board. This data was collected to mimic a standard gait assessment. Subjects were asked to

Table 2. Dataset Overview

Metric	Value
Number of Subjects	21
Number of Steps	2091
Number of Strides	1820
Male / Female	10/11
Age Range	21-35
Step time range (s)	0.47 - 0.80
Step length range (m)	0.48 - 0.85
Step width range (m)	0.49 - 0.87
Stride time range (s)	0.96 - 1.51
Stride length range (m)	0.97 - 1.69
Stride velocity range (m/s)	0.67 - 1.74
Cadence range (steps per minute)	87.52 - 122.03
Swing time range (s)	0.33 - 0.56
Stance time range (s)	0.59 - 1.02

walk at a comfortable pace over the walking mat and after each session the subject could choose to rest. The GAITRite was synchronised with our system using NTP to a local NTP server. This data was collected over a two week period at the School of Computing at the National University of Singapore. The results of the systems performance on this data follows in the next subsection.

8.2 Results

The results are split into four parts, one on the UWB data, one on the IMU data, one with a simple fusion model, and finally one on comparing and summarising the technologies. All of the methods in these preceding sections have been chosen as they are low time and space complexity and thus can be performed on the limited hardware available on wearable sensors.

8.2.1 UWB Methods. First we will look at the UWB-only methods for measuring gait metrics. Whilst there are undoubtedly some errors introduced due the simplification of the 3-dimensional nature of the physical system, this model performs well. Table 3 shows the root mean square error (RMSE), mean absolute error (MAE) and mean absolute percentage error (MAPE) of UWB measurements in comparison to the GAITRite. We can see across most metrics we are getting within 4-5% of the ground truth value. Additionally, we are measuring step width which is not a metric calculated by standard wearables. Despite the limitations of UWB measurement ranging technologies we are able to get accurate gait metrics.

8.2.2 IMU Methods. The simple IMU methods used in this paper do not perform as well as the UWB metrics. This is expected as these methods are low time-complexity, and relatively simplistic. Table 4 shows the root mean square error (RMSE), mean absolute error (MAE), and mean absolute percentage error (MAPE) of IMU measurements in comparison to the GAITRite. We can see the temporal measurements are very similar to the UWB methods, however the spatial metrics perform worse. These results are consistent with those from other

Table 3. Comparison of UWB measurements vs. GAITRite

Metric	RMSE	MAE	MAPE
Step Time (s)	0.016	0.012	2.14%
Stride Time (s)	0.016	0.011	1.01%
Step Width (m)	0.041	0.033	4.85%
Step Length (m)	0.041	0.032	4.75%
Stride Length (m)	0.070	0.056	4.11%
Stride Velocity (m/s)	0.067	0.051	4.23%
Cadence (steps/min)	0.703	0.442	0.42%
Swing Time (s)	0.029	0.022	5.17%
Stance Time (s)	0.030	0.022	3.07%

researchers using foot-mounted 6-axes IMU methods [34]. These IMU measurements though are not affected by line of sight as UWB measurements are and therefore we will now look at a simple fusion of the two methods.

Table 4. Comparison of IMU measurements vs. GAITRite

Method	Metric	RMSE	MAE	MAPE
3 & 6 Axes	Stride Time (s)	0.056	0.022	1.96%
3 Axes	Stride Length (m)	0.132	0.105	7.96%
6 Axes	Stride Length (m)	0.140	0.111	8.42%

8.2.3 Simple Fusion. Although it performs worse overall, the IMU can be more accurate in measuring the stride length in a subset of our dataset. This is likely due to the UWB sensors temporarily losing line of sight during a narrow step (recall the spike in Figure 10a). To take advantage of this, we combine our stride lengths using a linear sum of the length measurements from the two with the form,

$$Str_l = v_0 Str_l^{UWB} + v_1 Str_l^{IMU}.$$

We also try compensating for the slight difference in UWB stride length error between measuring the left and right strides by fitting this same model for the left and right strides independently. We can see an approximate 20% improvement in accuracy by combining the two with these methods in Table 5

Table 5. Simple Fusion of IMU and UWB vs. GAITRite

Method	Metric	RMSE	MAE	MAPE
Linear Combination	Stride Length (m)	0.064	0.050	3.72%
Linear Combination (Strides)	Stride Length (m)	0.063	0.050	3.70%

8.2.4 Summary. In summary, our system can measure gait metrics that are not possible on such IMU-based wearables, and we have also shown a way to get stable spatial readings of steps. We show how a combination of IMU and UWB can give an increase in accuracy. This system combines these two technologies for the benefits of both IMU systems and walking mats at a fraction of the cost. The GAITRite walking mat costs in the order of tens of thousands of dollars, whereas a set of four of these sensors is less than five hundred dollars (even before large scale manufacture). The sensors can also be precisely synchronised between themselves, and allow for accurate foot placement/stance estimation. Unlike the GAITRite mat, our system can give direct measurements of foot movement through the whole gait cycle, even when the feet are in motion and above the mat. This measurement throughout the whole gait cycle allows us to directly measure gait parameters such as stride length (as one foot passes by the other) rather than estimating it based on foot placement as the GAITRite does. In this next section, we will discuss future directions.

9 FUTURE WORK

An important area for consideration is the use of more complex sensor fusion algorithms, such as in the Kalman Filter fusion methods described in [40]. The geometry of our sensor system allows for some constraint-based models to be used. While the end goal is to have all of this computation executed onboard the chip, and therefore be completely portable, we will also look at the use of machine learning methods to improve the accuracy of our system.

In addition to their role in measuring distances, and precise time synchronisation, the UWB sensors can also be used for high speed intra-sensor communication. The data rate is high (6.5Mb/s), but other factors limit it to about 6000B/s in practice. Regardless, this is a significant amount of data, and raises the possibility of making much more use of the sensor network, say for example, fusing the data from the IMU sensors on each foot, and even between feet in real time. Furthermore, we are not limited to using these sensors in their current locations, they could be used on other extremities to measure different types of motion such as arm swing.

One limitation is the dataset used. Specifically, we would like to collect a large amount of data of elderly adults, to design better UWB algorithms for gait parameter estimation. Furthermore, direct comparisons with GAITRite are limited in that they are unable to capture foot motion in the air. We will look to motion capture technologies to serve as a ground truth for in-air measurements. Investigation into optimising the sampling and transmission rate of both UWB and IMU readings is also a non-trivial problem. Another limitation of this work is that our system does not measure all of the metrics available on the GAITRite mat such as base-of-support, double, and single support time. Additionally, the GAITRite mat has a higher sampling rate than our system (240Hz vs 100 Hz).

The use of UWB technology in wearables is not without its downsides and limitations. The main limitation is the power requirement of running a UWB radio, which unlike IMUs or pressure sensors, requires a substantive increase in current when in use. Another problem is the accuracy of the oscillators/timers in the UWB chip. They are limited in time resolution and therefore the distances that are measurable. Like any radio technology, UWB radios are susceptible to interference and may be affected in noisy areas such as near electrical sources. However, despite these limitations, we are able to measure some gait metrics with high accuracy when compared to the GAITRite mat.

10 CONCLUSIONS

In conclusion, we have shown a new wireless wearable sensor system which is capable of measuring important gait metrics not previously measurable in traditional IMU-based sensors. Step width variability in particular is predictive of fall risk and thus of great importance. Furthermore, we have demonstrated the ability of the sensors

to measure foot positions on step placement. This could be used to detect step abnormality. We also collected a dataset which includes time-synchronised ground truth GAITRite measurements.

Our system has a battery life of approximately two and a half hours when it is used continuously. This is sufficient for use in a clinical setting when compared with actual clinical walking gait assessment sessions which last approximately 10-15 minutes. In the data collection trials we conducted, the units only needed to be recharged at the end of a day's recording. The sensors themselves take approximately one hour to recharge. Our smartphone application can also be used to record data of our sensors even when outside the hospital or a clinical setting. Our system allows the user to be untethered and able to walk in any direction, unlike the GAITRite which only allows for straight line walking over an instrumented mat. The potential for these sensors to be used in different configurations to measure different types of body motion is also of great interest. The authors believe that this technology and configuration is promising and has merit for use in many fields including sports medicine, gait-based neurological diagnostics, fall risk assessment, and monitoring of the elderly.

ACKNOWLEDGMENTS

The authors would like to thank Dr. Chitralekha Gupta and Shiyao Zhu for their help in data collection. The authors would also like to thank the anonymous reviewers for their helpful and constructive comments. Lastly, we would like to thank all of the participants in our study. This project was partially funded by two research grants, C-251-000-065-001 from the Dean's Strategic Initiative, School of Computing, National University of Singapore and R-263-000-C54-114 from the Ministry of Education, Singapore.

REFERENCES

[1] M. Al-Amri, K. Nicholas, K. Button, V. Sparkes, L. Sheeran, and J. L. Davies. 2018. Inertial Measurement Units for Clinical Movement Analysis: Reliability and Concurrent Validity. *Sensors* 18, 719 (2018).

[2] A. Alarifi, A. Al-Salman, M. Alsaleh, A. Alnafessah, S. Al-Hadhrami, M. A. Al-Ammar, and H. S. Al-Khalifa. 2016. Ultra Wideband Indoor Positioning Technologies: Analysis and Recent Advances. *Sensors (Basel)* 16, 5 (05 2016).

[3] Boyd Anderson, Shenggao Zhu, Ke Yang, Jian Wang, Hugh Anderson, Chao Xu Tay, Vincent Y. F. Tan, and Ye Wang. 2018. MANA: Designing and Validating a User-Centered Mobility Analysis System. In *Proceedings of the 20th International ACM SIGACCESS Conference on Computers and Accessibility (ASSETS '18)*. ACM, New York, NY, USA, 321–332. https://doi.org/10.1145/3234695.3236340

[4] Arif Reza Anwary, Hongnian Yu, and Michael Vassallo. 2018. An Automatic Gait Feature Extraction Method for Identifying Gait Asymmetry Using Wearable Sensors. *Sensors* 18, 2 (2018). https://doi.org/10.3390/s18020676

[5] A. R. Anwary, H. Yu, and M. Vassallo. 2018. Optimal Foot Location for Placing Wearable IMU Sensors and Automatic Feature Extraction for Gait Analysis. *IEEE Sensors Journal* 18, 6 (March 2018), 2555–2567. https://doi.org/10.1109/JSEN.2017.2786587

[6] R. Bharadwaj, S. Swaisaenyakorn, C. G. Parini, J. C. Batchelor, and A. Alomainy. 2017. Impulse Radio Ultra-Wideband Communications for Localization and Tracking of Human Body and Limbs Movement for Healthcare Applications. *IEEE Transactions on Antennas and Propagation* 65, 12 (Dec 2017), 7298–7309. https://doi.org/10.1109/TAP.2017.2759841

[7] J. S. Brach, J. E. Berlin, J. M. VanSwearingen, A. B. Newman, and S. A. Studenski. 2005. Too much or too little step width variability is associated with a fall history in older persons who walk at or near normal gait speed. *J Neuroeng Rehabil* 2 (Jul 2005), 21.

[8] Julià Camps, Albert Samà Monsonís, Mario Martín, Daniel Rodríguez-Martín, Carlos Pérez, Sheila Alcaine, Berta Mestre, Anna Prats, Maria Cruz Crespo Maraver, Joan Cabestany, Angels Bayés, and Andreu Català. 2017. Deep Learning for Detecting Freezing of Gait Episodes in Parkinson's Disease Based on Accelerometers. 344–355. https://doi.org/10.1007/978-3-319-59147-6_30

[9] S. Chen, J. Lach, B. Lo, and G. Z. Yang. 2016. Toward Pervasive Gait Analysis With Wearable Sensors: A Systematic Review. *IEEE Journal of Biomedical and Health Informatics* 20, 6 (Nov 2016), 1521–1537.

[10] Kellen Garrison Cresswell, Yongyun Shin, and Shanshan Chen. 2017. Quantifying Variation in Gait Features from Wearable Inertial Sensors Using Mixed Effects Models. *Sensors* 17, 3 (2017). https://doi.org/10.3390/s17030466

[11] Farzin Dadashi, Benoit Mariani, Stephane Rochat, Christophe Büla, Brigitte Santos-Eggimann, and Kamiar Aminian. 2013. Gait and Foot Clearance Parameters Obtained Using Shoe-Worn Inertial Sensors in a Large-Population Sample of Older Adults. *Sensors (Basel, Switzerland)* 14 (12 2013), 443–57. https://doi.org/10.3390/s140100443

[12] Omid Dehzangi, Mojtaba Taherisadr, and Raghvendar ChangalVala. 2017. IMU-Based Gait Recognition Using Convolutional Neural Networks and Multi-Sensor Fusion. *Sensors* 17 (11 2017), 2735. https://doi.org/10.3390/s17122735

[13] S. Del Din, A. Godfrey, and L. Rochester. 2016. Validation of an Accelerometer to Quantify a Comprehensive Battery of Gait Characteristics in Healthy Older Adults and Parkinson's Disease: Toward Clinical and at Home Use. *IEEE Journal of Biomedical and Health Informatics* 20, 3 (May 2016), 838–847. https://doi.org/10.1109/JBHI.2015.2419317

[14] M. A. El-Nasr, H. Shaban, and R. M. Buehrer. 2011. Measurement and extraction of base-of-support gait parameter using a novel accurate human locomotiontracking system via UWB radios. In *2011 1st Middle East Conference on Biomedical Engineering*. 188–191. https://doi.org/10.1109/MECBME.2011.5752097

[15] D. Gaetano, P. McEvoy, M. J. Ammann, C. Brannigan, L. Keating, and F. Horgan. 2014. On-body fidelity factor for footwear antennas over different ground materials. In *The 8th European Conference on Antennas and Propagation (EuCAP 2014)*. 1410–1414. https://doi.org/10.1109/EuCAP.2014.6902044

[16] B. Großwindhager, C. A. Boano, M. Rath, and K. Römer. 2018. Concurrent Ranging with Ultra-Wideband Radios: From Experimental Evidence to a Practical Solution. In *2018 IEEE 38th International Conference on Distributed Computing Systems (ICDCS)*. 1460–1467. https://doi.org/10.1109/ICDCS.2018.00149

[17] J. Hamie, B. Denis, and M. Maman. 2014. On-body localization experiments using real IR-UWB devices. In *2014 IEEE International Conference on Ultra-WideBand (ICUWB)*. 362–367. https://doi.org/10.1109/ICUWB.2014.6959008

[18] J. Hannink, T. Kautz, C. F. Pasluosta, K. G. Gasmann, J. Klucken, and B. M. Eskofier. 2017. Sensor-Based Gait Parameter Extraction With Deep Convolutional Neural Networks. *IEEE Journal of Biomedical and Health Informatics* 21, 1 (Jan 2017), 85–93. https://doi.org/10.1109/JBHI.2016.2636456

[19] J. M. Hausdorff, D. A. Rios, and H. K. Edelberg. 2001. Gait variability and fall risk in community-living older adults: a 1-year prospective study. *Arch Phys Med Rehabil* 82, 8 (Aug 2001), 1050–1056.

[20] H. Jagos, K. Pils, M. Haller, C. Wassermann, C. Chhatwal, D. Rafolt, and F. Rattay. 2017. Mobile gait analysis via eSHOEs instrumented shoe insoles: a pilot study for validation against the gold standard GAITRite. *Journal of Medical Engineering & Technology* 41 (2017), 375–386. Issue 5.

[21] Y. Jiang and V. C. M. Leung. 2007. An Asymmetric Double Sided Two-Way Ranging for Crystal Offset. In *2007 International Symposium on Signals, Systems and Electronics*. 525–528. https://doi.org/10.1109/ISSSE.2007.4294528

[22] Antonio Ramón Jiménez, Fernando Seco, José Carlos Prieto, and J Guevara. 2010. Indoor pedestrian navigation using an INS/EKF framework for yaw drift reduction and a foot-mounted IMU. In *Positioning Navigation and Communication (WPNC), 2010 7th Workshop on*. IEEE, 135–143.

[23] R. Liu, C. Yuen, T. N. Do, D. Jiao, X. Liu, and U. X. Tan. 2017. Cooperative relative positioning of mobile users by fusing IMU inertial and UWB ranging information. In *2017 IEEE International Conference on Robotics and Automation (ICRA)*. 5623–5629. https://doi.org/10.1109/ICRA.2017.7989660

[24] Glenn MacGougan, Kyle O'Keefe, and Richard Klukas. 2009. Ultra-wideband ranging precision and accuracy. *Measurement Science and Technology* 20, 9 (2009), 095105. http://stacks.iop.org/0957-0233/20/i=9/a=095105

[25] A. Muro-de-la Herran, B. Garcia-Zapirain, and A. Mendez-Zorrilla. 2014. Gait analysis methods: an overview of wearable and non-wearable systems, highlighting clinical applications. *Sensors (Basel)* 14, 2 (Feb 2014), 3362–3394.

[26] E. Nordin, R. Moe-Nilssen, A. Ramnemark, and L. Lundin-Olsson. 2010. Changes in step-width during dual-task walking predicts falls. *Gait Posture* 32, 1 (May 2010), 92–97.

[27] W. Pirker and R. Katzenschlager. 2017. Gait disorders in adults and the elderly : A clinical guide. *Wien. Klin. Wochenschr.* 129, 3-4 (Feb 2017), 81–95.

[28] William Premerlani and Paul Bizard. 2009. *Direction Cosine Matrix IMU: Theory*. Technical Report.

[29] Y. Qi, C. B. Soh, E. Gunawan, K. S. Low, and A. Maskooki. 2014. A Novel Approach to Joint Flexion/Extension Angles Measurement Based on Wearable UWB Radios. *IEEE Journal of Biomedical and Health Informatics* 18, 1 (Jan 2014), 300–308. https://doi.org/10.1109/JBHI.2013.2253487

[30] John R. Rebula, Lauro V. Ojeda, Peter G. Adamczyk, and Arthur D. Kuo. 2013. Measurement of foot placement and its variability with inertial sensors. *Gait & Posture* 38, 4 (2013), 974 – 980. https://doi.org/10.1016/j.gaitpost.2013.05.012

[31] L Rubio, J Reig, Herman Fernández, and Vicent M. Rodrigo-Peñarrocha. 2013. Experimental UWB Propagation Channel Path Loss and Time-Dispersion Characterization in a Laboratory Environment. *International Journal of Antennas and Propagation* 2013 (03 2013). https://doi.org/10.1155/2013/350167

[32] H. A. Shaban, M. A. El-Nasr, and R. M. Buehrer. 2010. Toward a Highly Accurate Ambulatory System for Clinical Gait Analysis via UWB Radios. *IEEE Transactions on Information Technology in Biomedicine* 14, 2 (March 2010), 284–291. https://doi.org/10.1109/TITB.2009.2037619

[33] Manmohan Sharma, Clive Parini, and Akram Alomainy. 2015. UWB Sensor Nodes for Tracking of Human Motion in Medical and Rehabilitation Applications. In *Proceedings of the 5th EAI International Conference on Wireless Mobile Communication and Healthcare (MOBIHEALTH'15)*. ICST (Institute for Computer Sciences, Social-Informatics and Telecommunications Engineering), ICST, Brussels, Belgium, Belgium, 86–89. https://doi.org/10.4108/eai.14-10-2015.2261745

[34] Benoît Sijobert, Mourad Benoussaad, Jennifer Denys, Roger Pissard-Gibollet, Christian Geny, and Christine Azevedo-Coste. 2015. Implementation and Validation of a Stride Length Estimation Algorithm, Using a Single Basic Inertial Sensor on Healthy Subjects and Patients Suffering from Parkinson's Disease. *Health* 7 (06 2015), 704–714. https://doi.org/10.4236/health.2015.76084

[35] Yoonseon Song, Seungchul Shin, Seunghwan Kim, Doheon Lee, and Kwang Hyung Lee. 2007. Speed estimation from a tri-axial accelerometer using neural networks. In *Engineering in Medicine and Biology Society, 2007. EMBS 2007. 29th Annual International Conference of the IEEE*. IEEE, 3224–3227.

[36] S. Studenski, S. Perera, K. Patel, C. Rosano, K. Faulkner, M. Inzitari, J. Brach, J. Chandler, P. Cawthon, E. B. Connor, M. Nevitt, M. Visser, S. Kritchevsky, S. Badinelli, T. Harris, A. B. Newman, J. Cauley, L. Ferrucci, and J. Guralnik. 2011. Gait speed and survival in older adults. *JAMA* 305, 1 (Jan 2011), 50–58.

[37] Can Tunca, Nezihe Pehlivan, Nağme Ak, Bert Arnrich, Gülüstü Salur, and Cem Ersoy. 2017. Inertial Sensor-Based Robust Gait Analysis in Non-Hospital Settings for Neurological Disorders. *Sensors* 17, 4 (2017). https://doi.org/10.3390/s17040825

[38] Liang Wang, Wen Cheng, Lijia Pan, Tao Gu, Tianheng Wu, Xianping Tao, and Jian Lu. 2018. SpiderWalk: Circumstance-aware Transportation Activity Detection Using a Novel Contact Vibration Sensor. *Proc. ACM Interact. Mob. Wearable Ubiquitous Technol.* 2, 1, Article 42 (March 2018), 30 pages. https://doi.org/10.1145/3191774

[39] Tianben Wang, Zhu Wang, Daqing Zhang, Tao Gu, Hongbo Ni, Jiangbo Jia, Xingshe Zhou, and Jing Lv. 2016. Recognizing Parkinsonian Gait Pattern by Exploiting Fine-Grained Movement Function Features. *ACM Trans. Intell. Syst. Technol.* 8, 1, Article 6 (Aug. 2016), 22 pages. https://doi.org/10.1145/2890511

[40] Yan Wang and Xin Li. 2017. The IMU/UWB Fusion Positioning Algorithm Based on a Particle Filter. *ISPRS International Journal of Geo-Information* 6, 8 (2017). https://doi.org/10.3390/ijgi6080235

[41] Edward P. Washabaugh, Tarun Kalyanaraman, Peter G. Adamczyk, Edward S. Claflin, and Chandramouli Krishnan. 2017. Validity and repeatability of inertial measurement units for measuring gait parameters. *Gait & Posture* 55 (2017), 87 – 93. https://doi.org/10.1016/j.gaitpost.2017.04.013

[42] Shenggao Zhu, Hugh Anderson, and Ye Wang. 2012. A real-time on-chip algorithm for IMU-Based gait measurement. In *Advances in Multimedia Information Processing–PCM 2012*. Springer, 93–104.

[43] Wiebren Zijlstra. 2004. Assessment of spatio-temporal parameters during unconstrained walking. *European J Applied Physiology* 92, 1-2 (2004), 39–44.

[44] Wiebren Zijlstra and At L Hof. 2003. Assessment of spatio-temporal gait parameters from trunk accelerations during human walking. *Gait & Posture* 18, 2 (2003), 1–10.